*Geophys. J. R. astr. Soc.* (1977) 49, 357–370

# The effect of intrinsic oceanic upper-mantle heterogeneity on regionalization of long-period Rayleigh-wave phase velocities

Emile A. Okal *Seismological Laboratory, California Institute of Technology, Pasadena, California 91125, USA*

Received 1976 October 26; in original form 1976 August 25

**Summary.** Rayleigh-wave phase velocities at very long periods (185–290 s) are investigated and regionalized, taking into account the lateral heterogeneities within ocean plates revealed by earlier studies at shorter periods. The two-station method is applied to a few 'pure-age' oceanic paths, and is shown to be compatible with the average Earth model C2 (Anderson & Hart 1976) below depths of 180 km. Under this assumed oceanic model, regionalized for age above 180 km, continental velocities are then derived from a set of experimental great-circle values, both new or taken from previously published studies. The results basically agree with earlier studies (Dziewonski 1970; Kanamori 1970), although they exhibit less scatter than Kanamori's model. Results are successfully checked against a set of values derived by the two-station method from a pure continental path.

Although the shield velocities are substantially different from the mean oceanic ones, they still fall within the range of variation of oceanic velocities with the age of the plate. This makes velocities derived theoretically from Jordan's (1975a, b) models of deep continent–ocean lateral heterogeneities, inconsistent with the present set of experimental data. Finally, we show that Dziewonski's (1971) model S2 reconciles all experimental seismic data relative to shields, without being significantly different from oceanic models below 240 km.

## Introduction

In a series of recent papers, Jordan (1975a, b) and Sipkin & Jordan (1975, 1976) have proposed that lateral heterogeneities between oceans and continents extend to depths of 400 km, and possibly 600 km. Their conclusion is based on the study of *ScS* travel times, and on the discrepancy between models inverted from body- and surface-wave data. On the other hand, from a slightly different set of *ScS* data, Okal & Anderson (1975) have suggested that the travel-time differences between oceans and continents can be accounted for by the upper 180 km of crust and mantle. Furthermore, it has recently been shown (Liu, Anderson & Kanamori 1976; Anderson *et al.* 1977; Hart, Anderson & Kanamori 1976, 1977) that the discrepancy between inversions of body- and surface-wave data was due to anelasticity in the mantle. In view of these controversies, it is important to investigate whether or not a definite continent–ocean lateral heterogeneity is present in surface-wave phase velocities, at periods on the order of 200–300 s, whose values are substantially dependent on seismic velocities down to 600 km. Models recently derived from regionalization of surface-wave phase velocities (Toksöz & Anderson 1966; Dziewonski 1970; Kanamori 1970) generally exhibit continent–ocean lateral heterogeneities. Furthermore, Kanamori's results show a fairly large scatter in the differences between Rayleigh-wave phase velocities for oceans and shields, at 200–300 s.

However, at shorter periods, recent investigations of oceanic surface-wave phase velocities (Leeds, Kausel & Knopoff 1974; Kausel, Leeds & Knopoff 1974; Leeds 1975) have yielded a model of the evolution of the oceanic lithosphere, which is basically consistent with theoretical models derived from plate tectonics (Parker & Oldenburg 1973). This model shows that considerable lateral heterogeneities exist within the oceanic plates. This effect might be responsible for the scatter in Kanamori's results, which were obtained on the assumption of a uniform oceanic phase velocity, but from data sampling all ages of the oceanic lithosphere. This warrants a reassessment of continental phase velocities obtained from the pure-pathing method, as described by Toksöz & Anderson (1966), Dziewonski (1970) and Kanamori (1970). The object of the present paper is to carry out such a regionalization of Rayleigh-wave phase velocities, taking into account their variation with age across oceanic plates. In a detailed study of surface waves in the East Pacific, Forsyth (1975) recently confirmed the dependence of the velocities with the age of the plate, and also claimed that Love- and Rayleigh-wave data are inconsistent unless anisotropy is introduced in the upper mantle. However, in view of the very limited set of data available at long periods, and of the many different models which can explain the observed anisotropy, we decided not to take anisotropy into account in the present study.

In the first Section of this paper, we build up a table of theoretical Rayleigh-wave oceanic phase velocities, for several values of the age of the lithosphere, by assuming that the ocean below 180 km is similar to the gross earth model C2, as described by Anderson & Hart (1976). We then use a few 'pure-age' paths, in a two-station computation, to check the overall agreement of this model with local data. In Section 2, we then carry out a regionalization of dispersion curves, solving for pure-path continental values, and allowing for a variation of oceanic velocities with age, in accordance with the results from the first Section. Again, we make sure that the results agree with direct experimental values obtained from a pure continental path by the two-station method. In Section 3, we discuss the results and compare them with the two models proposed by Jordan (1975a) for continental and oceanic structure (with substantial differences down to 650 km). We prove the latter's incompatibility with the data. We also discuss Dziewonzki's (1971) shield models with respect to the recent vertical shear-wave data obtained from *ScS* studies.

## 1 Rayleigh-wave phase velocities from an oceanic model of aging lithosphere

Studies of Rayleigh-wave phase velocities at shorter periods ($T \leqslant 150$ s) have led Leeds and co-workers (Kausel *et al.* 1974; Leeds *et al.* 1974; Leeds 1975) to a seismic model of the evolution of the lithospheric plate with age in the Pacific Ocean. In the present study, we will assume that lateral heterogeneity under the ocean is confined to the upper 180 km, and that the remaining part of the mantle is identical to the average earth model C2. This way, we define eight different oceanic models (hereafter 'Ocean 1'–'Ocean 8'), corresponding to the eight regions defined in Leeds *et al.* (1974) (respectively 150, 120, 100, 70, 50, 30, 15 and 5-Myr old), after the three older regions have been corrected in accordance with Leeds'

**Table 1.** (a) Theoretical Rayleigh-wave phase velocities for oceanic models Ocean 1–Ocean 8.

| Model | Age (Myr) | Velocity (km/s) at period (s) 292.57 | 256.00 | 227.55 | 204.80 | 186.18 |
|---|---|---|---|---|---|---|
| 1 | 150 | 5.260 | 4.989 | 4.788 | 4.642 | 4.535 |
| 2 | 120 | 5.249 | 4.976 | 4.771 | 4.619 | 4.506 |
| 3 | 100 | 5.242 | 4.968 | 4.761 | 4.607 | 4.492 |
| 4 | 70 | 5.237 | 4.963 | 4.756 | 4.601 | 4.485 |
| 5 | 50 | 5.234 | 4.960 | 4.753 | 4.599 | 4.482 |
| 6 | 30 | 5.227 | 4.953 | 4.746 | 4.592 | 4.475 |
| 7 | 15 | 5.208 | 4.934 | 4.728 | 4.575 | 4.458 |
| 8 | 5 | 5.184 | 4.909 | 4.703 | 4.549 | 4.433 |

(b) Experimental oceanic values from the two-station method.

| | | | | | | |
|---|---|---|---|---|---|---|
| GUA–KIP | | * | 4.983 | 4.784 | 4.618 | 4.484 |
| SOM–KIP | | * | * | 4.729 | 4.577 | 4.455 |

* No substantial energy in the signal at these periods.

later paper (1975). We compute theoretical phase velocities at five standardized periods ($T$ = 292.57, 256.00, 227.55, 204.80 and 186.18 s), which are harmonics of the main fundamental 2048-s window, which will be used in all Fast-Fourier transform analyses in the present paper. Results are shown in Table 1(a), and on Fig. 1. Differences in velocities between younger and older oceans are on the order of 1.5–2 per cent, which is at least as large as the continental–oceanic differences reported in previous studies (Kanamori 1970; Dziewonski 1970).

Before proceeding any further, it is necessary to check these results against experimental values. The use of 200–300 s waves restricts the choice of the data to a fairly small number of events, in which energy is present at such periods. These are listed in Table 2. Furthermore, these are large earthquakes, for which, most of the time, no rupture mechanism accurate enough to allow the use of a one-station method, is available. A two-station

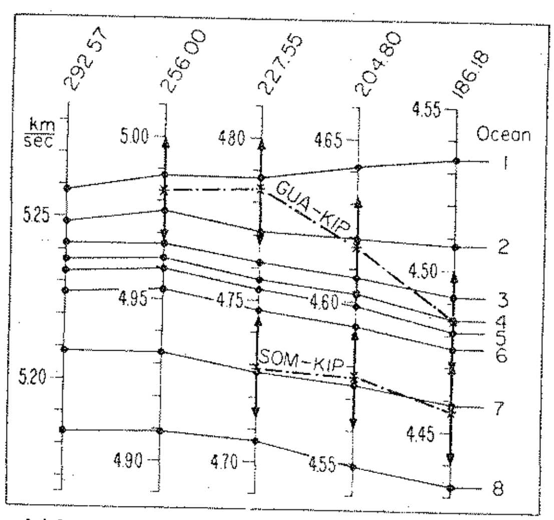


**Figure 1.** Theoretical Rayleigh-wave phase velocities for models 'Ocean 1'–'Ocean 8'. Different baselines are used at the five standard periods to eliminate the mean average dispersion. Superimposed are experimental data (asterisks) from the 'pure-age' paths SOM–KIP and KIP–GUA. The vertical arrows centred on them are error bars.

**Table 2.** Coordinates of earthquakes used in this study.

| Number | Name | Latitude °N | Longitude °E | Date |
|---|---|---|---|---|
| 1 | Rat Island | 51.3 | 178.55 | 4 Feb 65 |
| 2 | Alaska | 61.1 | -147.6 | 28 Mar 64 |
| 3 | Kurile | 44.8 | 149.5 | 13 Oct 63 |
| 4 | Niigata | 38.7 | 139.2 | 16 Jun 64 |
| 5 | Hindu-Kush | 36.4 | 70.7 | 14 Mar 65 |
| 6 | Mindanao | 6.5 | 126.6 | 2 Dec 72 |
| 7 | Mongolia | 45.2 | 99.2 | 4 Dec 57 |
| 8 | Assam | 28.4 | 96.7 | 15 Aug 50 |
| 9 | Moluccas | -2.4 | 126.0 | 24 Jan 65 |
| 10 | Chile | -38.0 | -73.5 | 22 May 60 |
| 11 | Colombia | -1.5 | -72.6 | 31 Jul 70 |
| 12 | Auckland Isl. | -49.1 | 164.2 | 12 Sep 64 |
| 13 | Kamchatka | 52.6 | 160.3 | 4 Nov 52 |
| 14 | Peru | -13.8 | -69.3 | 15 Aug 63 |

investigation is therefore necessary. Among the eathquakes listed in Table 2, the only two-station combination sampling only young (respectively old) ocean and providing a strong signal at the adequate periods, is: SOM–KIP (Hindu–Kush event) (respectively: GUA–KIP (Colombia event)) – see Fig. 2. Vertical WWSSN records from these stations were digitized over 2048 s and Fourier analysed. The phase velocity was computed from the classical formula (Toksöz & Ben-Menahem 1963)

$$c = (\Delta_2 - \Delta_1)/\{t_2 - t_1 + T\cdot[(\phi_2 - \phi_1)/2\pi + (n/4) + N]\}. \tag{1}$$

Here, $c$ is the phase velocity at period $T$, the $\Delta$'s are the distances travelled by the surface wave to stations 1 and 2, $t_1$ and $t_2$ are the initial times of the windows used in the process, $\phi_1$ and $\phi_2$ are the observed spectral phases (in radians), at period $T$, $n$ is the total number of epicentral and antipodal crossings between stations 1 and 2, and $N$ is a suitable integer. The accuracy of the data is on the order of twice the digitizing unit (2 s) in time, or 0.01 km/s for $c$. Results are shown in Table 1(b). Most of the SOM–KIP trace samples the Chile rise separating the Antarctica and Nazca plates (region 8), then the East Pacific Rise (regions 7 and 8), and finally young lithosphere (mostly regions 6 and 5). The average would then be expected to resemble models 'Ocean 6' or 'Ocean 7'. On the other hand, the GUA–KIP path samples the older parts of the Pacific Ocean (even possibly older than 150 Myr) (regions 1, 2, 3), and should then resemble models 'Ocean 1' or 'Ocean 2'. As can be seen from Table 1(a) and (b), and from Fig. 1, the results agree with these expectations. Thus, these experimental data given evidence that lateral heterogeneity within the Pacific plate is important at periods of 200–300 s, and is fairly well accounted for by models 'Ocean 1'–'Ocean 8'. This suggests that there is no need to extend the oceanic lateral heterogeneity below 180 km. This, indeed, is what most theories of plate tectonics predict, and also agrees

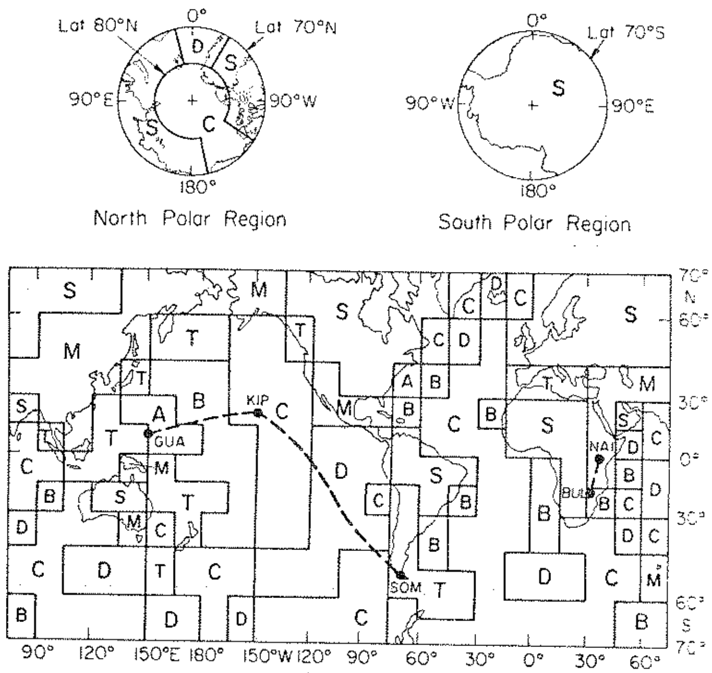


**Figure 2.** Map of the regionalization grid of the Earth used in Section 2. Labels A, B, C, D, T, M and S are explained in text. Also shown are the paths used for the two-station computations: GUA–KIP, KIP–SOM and BUL–NAI.

with the results of Okal & Anderson (1975). These authors were able to account for variations in multiple-*ScS* travel-time residuals across oceanic lithosphere by models whose heterogeneity was confined to the upper 180 km of the Earth. This result also allows us to assume from now on in this study that oceanic Rayleigh-wave phase velocities and their variation with the age of the plate are known.

## 2 Continental velocities: regionalization of Rayleigh-wave phase velocities allowing for lateral heterogeneity in the Oceanic Lithosphere

Unfortunately, it was not possible to isolate data to be processed by the two-station method over a pure shield path. Apart from the general distribution of stations and of the events listed in Table 2, one additional reason may be the smaller size of the continents, relative to the oceans, which makes both the numerator and the denominator in equation (1) smaller, yielding very inaccurate values of $c$. Consequently, regionalization of great-circle phase velocities appears to be necessary to obtain pure-path values of Rayleigh-wave phase velocities at periods larger than 180 s. In this Section, we carry out such a regionalization, allowing for the observed lateral heterogeneity in the oceanic lithosphere.

### 2.1 DATA SET

The data used in this Section includes both new data and data taken from previously published studies, which were interpolated to our standard periods. Table 3(a) lists the new data set, obtained from records analysed in the present study. Records of the Kamchatka earthquake at Pasadena, were from the north–south component of the high-gain strain

**Table 3.** (a) Experimental Rayleigh-wave phase velocities for great-circle paths obtained in the present study.

| Event, station and phases used. | | | Velocities (km/s) at Periods (s) | | | | |
|---|---|---|---|---|---|---|---|
| | | | 292.57 | 256.00 | 227.55 | 204.80 | 186.18 |
| 1 | HLW | R5 – R9 | 5.235 | 4.952 | 4.753 | 4.603 | * |
| 1 | SOM | R4 – R6 | 5.237 | 4.953 | 4.754 | 4.602 | 4.482 |
| 1 | CTA | R5 – R9 | * | 4.972 | 4.771 | 4.621 | * |
| 2 | SPA | R3 – R5 | 5.246 | 4.966 | 4.764 | 4.612 | 4.497 |
| 2 | AFI | R5 – R7 | 5.234 | 4.945 | 4.750 | 4.604 | 4.498 |
| 2 | RAB | R5 – R7 | * | 4.984 | 4.772 | 4.617 | 4.499 |
| 2 | GUA | R5 – R7 | * | 4.967 | 4.761 | 4.615 | 4.504 |
| 3 | GUA | R5 – R7 | 5.221 | 4.929 | 4.687 | 4.550 | 4.461 |
| 4 | GIE | R2 – R4 | 5.242 | 4.967 | 4.766 | 4.602 | 4.490 |
| 13 | PAS | R2 – R4 | 5.227 | 4.959 | 4.757 | 4.616 | 4.488 |

* No substantial energy in the signal at these periods.

(b) Additional data taken from the literature.

| Event No. | Station | Ref. | Phase velocity (km/s) at Period (s) | | | | |
|---|---|---|---|---|---|---|---|
| | | | 292.57 | 256.00 | 227.55 | 204.80 | 186.18 |
| 2 | PAS | b † | 5.231 | 4.954 | 4.746 | * | * |
| 3 | MDS | c | 5.243 | 4.962 | 4.760 | 4.604 | 4.437 |
| 3 | AAE | d † | 5.234 | 4.952 | 4.750 | 4.598 | 4.488 |
| 3 | ADE | d † | 5.246 | 4.975 | 4.774 | 4.613 | 4.499 |
| 3 | AFI | d † | 5.239 | 4.963 | 4.763 | 4.616 | 4.508 |
| 3 | HNR | d † | 5.240 | 4.972 | 4.767 | 4.612 | 4.500 |
| 3 | SHI | d † | 5.223 | 4.952 | 4.742 | 4.595 | * |
| 3 | TOL | d † | 5.238 | 4.969 | 4.766 | 4.615 | 4.501 |
| 7 | PAS | e † | * | 4.954 | 4.746 | 4.592 | 4.485 |
| 8 | PAS | e † | 5.232 | 4.955 | 4.745 | 4.598 | 4.489 |
| 9 | PAS | f † | 5.246 | 4.952 | 4.751 | 4.604 | 4.492 |
| 10 | PAS | g † | 5.240 | 4.960 | 4.754 | 4.596 | 4.476 |
| 12 | PAS | f † | 5.238 | 4.956 | 4.746 | 4.592 | 4.479 |
| 14 | GDH | h | 5.223 | 4.955 | 4.754 | 4.607 | 4.491 |
| 14 | NUR | h | 5.232 | 4.959 | 4.754 | 4.604 | 4.491 |
| 14 | MAL | h | 5.239 | 4.967 | 4.763 | 4.611 | 4.497 |
| 14 | AFI | h | 5.241 | 4.964 | 4.757 | 4.604 | 4.491 |
| 14 | ALQ | h | 5.231 | 4.961 | 4.755 | 4.602 | 4.485 |
| 14 | AAM | h | 5.232 | 4.960 | 4.759 | 4.611 | 4.497 |

* No data reported at those periods.

† Data used in Kanamori's [1970] solution.

instrument. All other records were from vertical long-period WWSSN instruments. In the case of the Rat Island earthquake (event 1), a strong aftershock interferes with most of the records of $R_7$. Therefore, $R_9$ is used together with $R_5$ at stations CTA and HLW. Table 3(b) similarly lists the additional data obtained from the literature.

### 2.2 REGIONALIZATION

Regionalization of the Earth was carried out by partitioning its surface into 248 cells: a 15-degree grid, both in latitude in longitude, was used, with special adjustments made in the polar regions. The areas of the various cells are not all equal, but the present partitioning of the Earth was found to be most convenient for rapid computer regionalization of great-circle paths. Only four different oceanic regions were considered. They are labelled A, B, C and D: A includes regions older than 135 Myr, and model A is taken as identical to 'Ocean 1'. B ranges from 135 to 80 Myr, and model B is an average of models 'Ocean 2 and 3'. C ranges from 80 to 30 Myr, and model C is an average of models 'Ocean 3, 4, 5 and 6'. D ranges from 30 Myr to 0, with model D averaging models 'Ocean 6, 7 and 8'. An attempt was initially made, using a much finer grid, to resolve all eight regions defined in Leeds' study. However, considering the wavelengths used in the present study (all larger than 830 km), this was found unnecessarv

Continents were divided into shields (region S) and Phanerozoic mountainous areas (region M). Trenches and marginal seas were kept as a separate entity (region T). Ages of the oceanic lithosphere were taken from the *Map of the age of the oceans* published by the Geological Society of America (1974). A computer program was written, which samples any great-circle path at 500-km intervals, and computes the percentage of its length falling into the seven different regions. The results are listed in Table 4.

### 2.3 SOLVING FOR CONTINENTAL VELOCITIES

At each of the five standardized periods ($T$), we solve the system of equations

$$\sum_j x_{ij}/v_j(T) = 1/c_i(T) \qquad (2)$$

for $v_S$, $v_M$ and $v_T$, using a least-square technique. Here $j$ = A, B, C, D, T, M, S is the index of the region; $i$ is the index of the path; $x_{ij}$ is the fraction of path $i$ lying in region $j$, and $c_i(T)$ is the observed phase velocity at period $T$ along great-circle $i$. Rather than solving for all seven $v_j$'s, we fix $v_A$, $v_B$, $v_C$ and $v_D$ to their known values obtained in Section 1, listed in Table 5(a), and solve only for $v_S$, $v_M$, $v_T$. This has the effect of reducing the number of unknowns, in view of the relatively small amount of data available. In so doing, we are ignoring the phase delays introduced along the path by heterogeneities elsewhere in the Earth, as discussed by Madariaga & Aki (1972). We are then seeking to explain the differences between Kanamori's and Dziewonski's models merely in terms of pure-path phase velocities.

Another objection to the use of equations (2) was Dahlen's (1975) suggestion that deep lateral heterogeneities in the mantle could cause variations as large as 0.2 per cent in the apparent great-circle path lengths. However, Dziewonski & Sailor (1976) and Dahlen (1976)

*References to Tables 3(b) and 4.*

a This study
b Toksöz & Anderson (1966)
c Abe, Sato & Frez (1970)
d Kanamori (1970)
e Toksöz & Ben-Menahem (1963)
f Ben-Menahem (1965)
g Anderson, Ben-Menahem & Archambeau (1965)
h Dziewonski (1970)

**Table 4.** Percentage of great-circle paths lying in each of the seven regions.

| Event | Station | Ref. | A | B | C | D | T | M | S |
|---|---|---|---|---|---|---|---|---|---|
| 1 | HLW | a | 0.00 | 25.00 | 16.25 | 10.00 | 5.00 | 8.75 | 35.00 |
| 1 | SOM | a | 0.00 | 7.50 | 32.50 | 23.75 | 17.50 | 18.75 | 0.00 |
| 1 | CTA | a | 8.75 | 5.00 | 41.25 | 11.25 | 7.50 | 10.00 | 16.25 |
| 2 | PAS | b | 0.00 | 0.00 | 28.75 | 26.25 | 10.00 | 26.25 | 8.75 |
| 2 | SPA | a | 0.00 | 3.75 | 52.50 | 3.75 | 0.00 | 18.75 | 21.25 |
| 2 | AFI | a | 0.00 | 17.50 | 27.50 | 10.00 | 7.50 | 3.75 | 33.75 |
| 2 | RAB | a | 7.50 | 16.25 | 40.00 | 11.25 | 5.00 | 3.75 | 16.25 |
| 2 | GUA | a | 10.00 | 10.00 | 32.50 | 7.50 | 13.75 | 6.25 | 20.00 |
| 3 | GUA | a | 3.75 | 3.75 | 30.00 | 8.75 | 13.75 | 11.25 | 28.75 |
| 3 | MDS | c | 0.00 | 5.00 | 40.00 | 3.75 | 25.00 | 8.75 | 17.50 |
| 3 | AAE | d | 0.00 | 27.50 | 23.75 | 10.00 | 2.50 | 22.50 | 13.75 |
| 3 | ADE | d | 3.75 | 3.75 | 31.25 | 6.25 | 13.75 | 10.00 | 31.25 |
| 3 | AFI | d | 3.75 | 23.75 | 20.00 | 7.50 | 13.75 | 8.75 | 22.50 |
| 3 | HNR | d | 8.75 | 8.75 | 31.25 | 3.75 | 18.75 | 6.25 | 22.50 |
| 3 | SHI | d | 0.00 | 26.25 | 26.25 | 6.25 | 5.00 | 18.75 | 17.50 |
| 3 | TOL | d | 7.50 | 12.50 | 26.25 | 2.50 | 17.50 | 5.00 | 28.75 |
| 4 | GIE | a | 0.00 | 5.00 | 31.25 | 23.75 | 23.75 | 15.00 | 1.25 |
| 7 | PAS | e | 0.00 | 0.00 | 30.00 | 26.25 | 8.75 | 26.25 | 8.75 |
| 8 | PAS | e | 0.00 | 1.25 | 31.25 | 23.75 | 11.25 | 31.25 | 1.25 |
| 9 | PAS | f | 5.00 | 21.25 | 38.75 | 3.75 | 18.75 | 1.25 | 11.25 |
| 10 | PAS | g | 2.50 | 0.00 | 37.50 | 25.00 | 11.25 | 12.50 | 11.25 |
| 12 | PAS | f | 0.00 | 15.00 | 30.00 | 8.75 | 11.25 | 27.50 | 7.50 |
| 13 | PAS | a | 1.25 | 8.75 | 30.00 | 23.75 | 20.00 | 16.25 | 0.00 |
| 14 | GDH | h | 3.75 | 5.00 | 23.75 | 3.75 | 16.25 | 16.25 | 31.25 |
| 14 | NUR | h | 1.25 | 1.25 | 31.25 | 12.50 | 28.75 | 7.50 | 17.50 |
| 14 | MAL | h | 7.50 | 17.50 | 31.25 | 7.50 | 21.25 | 5.00 | 10.00 |
| 14 | AFI | h | 1.25 | 12.50 | 21.25 | 8.75 | 12.50 | 11.25 | 32.50 |
| 14 | ALQ | h | 0.00 | 6.25 | 32.50 | 15.00 | 8.75 | 12.50 | 25.00 |
| 14 | AAM | h | 0.00 | 11.25 | 17.50 | 3.75 | 15.00 | 20.00 | 32.50 |

recently showed that this result was in error and agreed on a much smaller value, on the order of only 1/150 of 1 per cent. This effect is therefore totally negligible, given the accuracy of the present data.

The results of our solution are shown in Table 5(b) and on Fig. 3. Root-mean square residuals are on the order of 0.5 per cent. The immediate conclusions are:

(i) Shields and mountainous regions exhibit velocities generally in agreement with Dziewonski's results.

(ii) The dispersion curve obtained for shields is much smoother than Kanamori's.

(iii) Velocities for continents fall into the range of oceanic velocities: shield velocities are on the order of those of 30-Myr old oceanic mantle at 292 s, and of 100-Myr old ocean around 200 s.

Although no data was available for a direct test of shield velocities, a convenient alignment was found for a purely tectonic continental area: BUL–NAI (Rat Island Event),

**Table 5.** (a) Rayleigh-wave phase velocities used in models A, B, C, D when solving for models T, M, S.

| Model | Velocities (km/s) at periods (s) 292.57 | 256.00 | 227.55 | 204.80 | 186.18 |
|---|---|---|---|---|---|
| A | 5.259 | 4.989 | 4.788 | 4.642 | 4.535 |
| B | 5.246 | 4.972 | 4.766 | 4.613 | 4.499 |
| C | 5.236 | 4.961 | 4.754 | 4.600 | 4.483 |
| D | 5.206 | 4.932 | 4.726 | 4.572 | 4.455 |

(b) Solution for Rayleigh-wave phase velocities in regions T, M, S.

| | | | | | |
|---|---|---|---|---|---|
| T | 5.279 | 4.989 | 4.804 | 4.644 | 4.522 |
| M | 5.202 | 4.941 | 4.712 | 4.575 | 4.466 |
| S | 5.223 | 4.948 | 4.742 | 4.598 | 4.499 |

(c) Experimental continental Rayleigh-wave phase velocities from the two-station method.

| | | | | | |
|---|---|---|---|---|---|
| BUL–NAI | 5.199 | 4.940 | 4.690 | 4.591 | * |

* No substantial energy in the signal at this period.

(d) Solution for Rayleigh-wave phase velocities using only data used by Kanamori (1970) – † in Table 3(b).

| | | | | | |
|---|---|---|---|---|---|
| M | 5.213 | 4.954 | 4.724 | 4.571 | 4.488 |
| S | 5.223 | 4.978 | 4.780 | 4.629 | 4.527 |

(e) Theoretical Rayleigh-wave phase velocities for Jordan's oceanic and continental models.

| | | | | | |
|---|---|---|---|---|---|
| Oceanic model | 5.148 | 4.874 | 4.673 | 4.526 | 4.417 |
| Continental model | 5.259 | 5.000 | 4.808 | 4.667 | 4.561 |

sampling the African Rift over a length of 3200 km. Rayleigh-wave phase velocities obtained from these records by the two-station method are shown in Table 5(c). As the distance is shorter between BUL and NAI than distances used in Section 1 for oceanic paths, the precision is only about 0.02 km/s, but the agreement with the velocities obtained from equations (2) for region M is still excellent.

## 3 Discussion

Before discussing the results of the previous Section with respect to Dziewonski's and Kanamori's, it is worth noting the velocities obtained for the trench areas (region T). These are definitely larger than the corresponding average oceanic values. Again, for lack of data over sufficiently long paths, we were unable to check this observation by the two-station method. However, it is worth noting that a surface wave at 200–300 s, travelling over the area with a wavelength of 800–1500 km, will sample both the adjoining lithosphere, which is the oldest and fastest part of the ocean, and, at depth, the downgoing slab. The latter has been shown, both experimentally (Utsu 1967; Katsumata 1970; Isacks & Molnar 1971) and theoretically (Toksöz, Minear & Julian 1971) to be an area of higher seismic velocities. It may be that these effects dominate the low-velocity areas of partial melting which accompany the slab.

We first want to compare our results with Dziewonski's and Kanamori's. Our shield and mountain velocities basically agree with Dziewonski's, and they exhibit a behaviour somewhat different from those of Kanamori (see Fig. 3). As both data sets were used in the present inversion, these discrepancies require an explanation. Table 4 shows that Kanamori's paths sample more ocean than Dziewonski's (56 per cent of the paths versus 47 per cent).

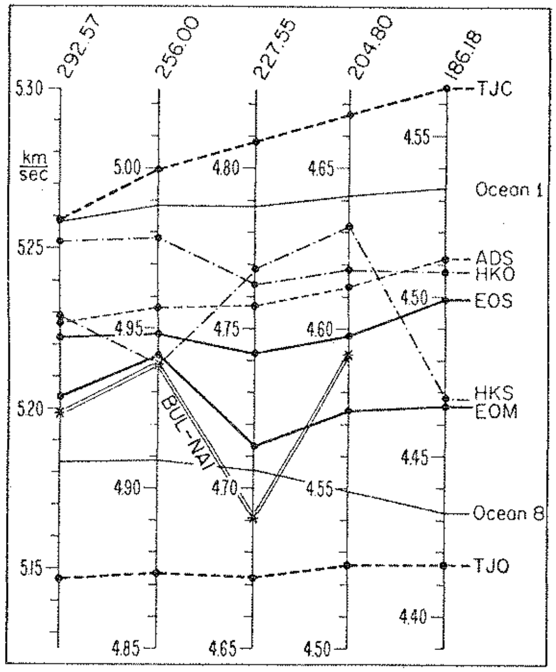


**Figure 3.** Regionalized Rayleigh-wave phase velocities obtained for shield (EOS) and mountainous areas (EOM) in the present study, as compared to Dziewonski's shield values (ADS), Kanamori's shield and ocean values (HKS and HKO). Also shown are Jordan's oceanic (TJO) and continental (TJC) models, uncorrected for $Q$. Models 'Ocean 1' and 'Ocean 8' are reproduced to show the range of variation of oceanic velocities. The vertical scales are as in Fig. 1. Superimposed is the experimental data from the 'pure' path BUL–NAI, obtained by the two-station method.

More importantly, the distribution of these oceanic paths among regions A, B, C, D is far from constant: for example, the Kurile–AFI great-circle path falls 27.5 per cent into the fast regions A and B, and 27.5 per cent into the slow regions C and D. Meanwhile Alaska–PAS falls 0 per cent into A and B, and 55 per cent into C and D. Similarly, Mongolia–PAS falls 0 per cent into A and B, and 56.2 per cent into C and D. Conversely, Dziewonski's paths are much more similar to each other. In terms of the solution of the least-square system under the assumption of only one oceanic velocity at each period, Kanamori's paths will be more unstable than Dziewonski's. We think that the larger diversity of the oceanic paths in Kanamori's data was responsible for the apparent scattering of his shield velocities, and for the discrepancy which exists between his results and Dziewonski's, especially around 180 s.

This can be checked by solving equations (2), using only the data used in Kanamori (1970), as identified in Table 3(b) by a dagger (†). The results of this test are listed in Table 5(d). Although the obtained shield values are somewhat higher than those from both this study and Dziewonski's, their trend is much less dispersive than Kanamori's (1970) solution. Values obtained for the mountainous areas are also in good agreement with those from both the present inversion – Table 5(b) – and the two-station investigation – Table 5(c).

Having investigated a range of oceanic models and confirmed Dziewonski's shield values in view of intrinsic oceanic heterogeneity, we will now discuss the phase velocities obtained from the two models proposed by Jordan (1975a), for continental and oceanic mantles. These two models differ to depths on the order of 650 km. Theoretical values computed from Jordan's oceanic and continental models are listed in Table 5(e). At this point, it should be noted that nowhere in the present study has the effect of anelasticity – as pointed out by Liu *et al.* (1976) – been taken into account in the computation of surface-wave phase velocities. However, both Leeds' models and model C2 were obtained from inversions of surface-wave data, which did *not* take this effect into account. Therefore direct comparison is possible, since the $Q$ correction would have the same effect on both experimental and theoretical velocities. On the other hand, Jordan's models are primarily body-wave models, obtained to match discrepancies reported from travel-time analyses. Therefore, a correction for the frequency dependence of elastic moduli caused by $Q$ should be included before comparing Jordan's models to values obtained from surface-wave data. Hart *et al.* (1977) recently reported that, at the periods involved (180–300 s), the $Q$ correction for spheroidal modes is on the order of 1 per cent, which means that phase velocities derived uncorrected from surface-wave data are about 0.05 km/s slow. Conversely, the correction to be applied to phase velocities derived from body-wave models, such as Jordan's, in order to compare them to velocities from the present study, is on the order of −0.05 km/s. As shown in Table 5 and Fig. 3, this correction makes Jordan's continental model basically consistent with experimental shield data, as obtained from this study, or Dziewonski's. However, a similar correction will move the oceanic values (curve 'TJO' on Fig. 3) still further away from the experimental data from any part of the ocean. Although in Jordan's own words, the two models which he describes are only tentative, the important point is the difference between them, which he reports to be warranted by body-wave data. Such a difference at a substantial depth (on the order of 600 km) will always lead to large continent–ocean surface-wave phase-velocity differences, regardless of the global average value.

In a recent paper, Sipkin & Jordan (1976) state that the 'baseline discrepancy' between continents and oceans can be explained in terms of a different value of $Q$ under oceans and continents. The maximum possible lateral variation in $Q$ would consist of a perfectly elastic oceanic mantle ($Q = \infty$) and of an anelastic continental mantle. (In fact, Kanamori (1970) reports no such definite behaviour in the attenuation of surface waves, and this model is just unrealistic.) Even so, using this hypothetical model to correct continental velocities, and keep oceanic ones uncorrected, Fig. 3 shows that we are left with an average difference between them of 0.07 km/s, and we are unable to reconcile the two models with the experimental data. Therefore, we conclude that the models of Jordan and Sipkin & Jordan are incompatible with the present available Rayleigh-wave phase-velocity data in the range 200–300 s.

Finally, we want to discuss the models which were derived by Dziewonski (1971) from his sets of oceanic and shield velocities, with respect to the data available at shorter periods and from body-wave studies. We have first computed Rayleigh-wave phase velocities for Dziewonski's (1971) shield models S1 and S2, at periods of 60 and 100 s. Results are reported in Table 6. Models S1 and S2 are totally compatible with the experimental data reported by Brune & Dorman (1963) over Canadian shield, and by Noponen (1966) for Finnish shield. The models also agree with Kanamori & Abe's (1968) recomputation of theoretical phase velocities from model CANSD, allowing for the curvature of the Earth, and for gravity at $T > 70$ s. Jordan's (1975a) continental model yields phase velocities substantially lower at 60 s, higher at 100 s, thereby exhibiting a dispersion between 60 and 100 s not in agreement with either of the experimental sets of shield data.

Although the term 'shield' is used in various studies with a somewhat variable meaning – as pointed out by Dziewonski (1971) – it is noteworthy to confirm the basic compatibility of Dziewonski's models S1 and S2 with data at shorter period.

Both Okal & Anderson (1975) and Sipkin & Jordan (1976) have reported one-way vertical shear-wave travel-time residuals for shield on the order of −2 s, with respect to the Jeffreys–Bullen tables. Okal & Anderson also report a +1 s residual for average (50–

Table 6. Theoretical (T) and experimental (E) Rayleigh-wave phase velocities at shorter periods.

| Model | Reference | Velocity (km/s) at 60 s | 100 s |
|---|---|---|---|
| S1 | Dziewonski (1971) (T) | 4.151 | 4.208 |
| S2 | Dziewonski (1971) (T) | 4.161 | 4.191 |
| CANSD | Kanamori & Abe (1968) (T) | 4.161 | 4.230 |
| Continental | Jordan (1975a) (T) | 4.129 | 4.221 |
| Canadian | Brune & Dorman (1963) (E) | 4.155 | 4.202 |
| Finland | Noponen (1966) (E) | 4.18 | * |

* No data reported at 100 s.

70 Myr old) ocean. We have computed residuals with respect to Jeffreys–Bullen for the top 620 km of Dziewonski's models O1 (+1.9 s), S1 (1.0 s) and S2 (–1.0 s). As explained earlier in this paper, a correction for $Q$ should be applied to these values, obtained from surface-wave models, before comparing them with body-wave data, such as the one derived from the Jeffreys–Bullen tables. This correction is on the order of –1.1 s (Hart *et al.* 1977). We end up with the following residuals: O1: +0.8 s; S1: –0.1 s; S2: –2.1 s.

Therefore, we conclude that Dziewonski's shield model S2 reconciles (a) body-wave travel-time residuals; (b) short-period Rayleigh-wave data; and (c) long-period surface-wave data. Model S1 (which has no low-velocity zone) provides an excellent fit to (b) and (c), but stays somewhat slow in terms of body waves. Although a more accurate description of the oceanic mantle is given by Leeds' various models, Dziewonski's model O1 is compatible with both average oceanic body-wave data, and with long-period surface-wave data. Thus, it is possible, through models O1 and S2, which differ insignificantly (less than 0.7 per cent) below 240 km, to fully account for all presently available seismic data individualizing continents and oceans. These data do not warrant strong lateral heterogeneities (on the order of 0.13 km/s or 2.7 per cent in Jordan's models), between oceans and continents at depths greater than 250 km.

## Conclusion

Our results can be summarized as follows:

(i) Oceanic models at depths shallower than 180 km, developed from the study of short-period Rayleigh-wave phase velocities, combined with the average model C2 at greater depths, correctly predict longer period (200–300 s) oceanic phase velocities, and their variations with the age of the plate, which can be as high as 2.5 per cent.

(ii) Such intrinsic oceanic inhomogeneities may create scatter in the dispersion curves, if not taken into account when regionalizing great-circle data for 'pure-path' phase velocities. When these heterogeneities are taken into account, continental velocities are found to be in agreement with Dziewonski's values, obtained from paths sampling the oceanic lithosphere fairly regularly.

(iii) Rayleigh-wave phase velocities for continental areas (both shields and mountainous regions) fall within the range of oceanic models, and the difference between average oceanic and continental velocities is on the same order of magnitude as the variation within the oceanic plate due to its age. This is incompatible with Jordan's models of strong, deep lateral heterogeneities between oceans and continents.

(iv) Dziewonski's (1971) shield model S2 reconciles all presently available experimental data for shields (body-wave, short- and long-period surface wave) without any substantial structural difference below 240 km with the average oceanic model O1.

## Acknowledgments

I am grateful to Professors D. L. Anderson, H. Kanamori and J. B. Minster, and to Seth Stein and Robert Geller for discussion over an earlier draft of this paper. R. S. Hart, D. L. Anderson, H. Kanamori, H. P. Liu, S. Sipkin and T. H. Jordan kindly provided preprints of their works in advance of publication. This work was supported by the Advanced Research Projects Agency of the Department of Defense, and was monitored by the Air Force Office of Scientific Research under contract F-44620-72-C-0078.

## References

Abe, K., Sato, Y. & Frez, J., 1970. Free oscillations of the Earth excited by the Kurile Island earthquake (1963), *Bull. earthq. Res. Inst. (Tokyo)*, **48**, 87–114.

Anderson, D. L., Ben-Menahem, A. & Archambeau, C. B., 1965. Attenuation of seismic energy in the upper mantle, *J. geophys. Res.*, **70**, 1441–1448.

Anderson, D. L. & Hart, R. S., 1976. An earth model based on free oscillations and body waves, *J. geophys. Res.*, **81**, 1461–1475.

Anderson, D. L., Kanamori, H., Hart, R. S. & Liu, H. P., 1977. The Earth as a seismic absorption band, *Science*, in press.

Ben-Menahem, A., 1965. Observed attenuation and *Q* values of seismic surface waves in the upper mantle, *J. geophys. Res.*, **70**, 4641–4651.

Brune, J. & Dorman, J., 1963. Seismic waves and Earth structure in the Canadian shield, *Bull. seism. Soc. Am.*, **53**, 167–210.

Dahlen, F. A., 1975. The correction of great-circular surface wave phase velocity measurements for the rotation and ellipticity of the Earth, *J. geophys. Res.*, **80**, 4895–4903.

Dahlen, F. A., 1976. Reply (to Dziewonski and Sailor), *J. geophys. Res.*, **81**, 4951.

Dziewonski, A. M., 1970. On regional differences in dispersion of surface waves, *Geophys. J. R. astr. Soc.*, **22**, 289–325.

Dziewonski, A. M., 1971. Upper mantle models from 'pure-path' dispersion data, *J. geophys. Res.*, **76**, 2587–2601.

Dziewonski, A. M. & Sailor, R. V., 1976. On the effect of the Earth's ellipticity on velocity of mantle waves, *J. geophys. Res.*, **81**, 4947–4950.

Forsyth, D. W., 1975. The early structural evolution and anisotropy of the oceanic upper mantle, *Geophys. J. R. astr. Soc.*, **43**, 103–162.

Geological Society of America, 1974. *The age of the ocean basins* (Map).

Hart, R. S., Anderson, D. L. & Kanamori, H., 1976. Shear velocity and density of an attenuating Earth, *Earth planet. Sci. Lett.*, **32**, 25–34.

Hart, R. S., Anderson, D. L. & Kanamori, H., 1977. The effect of attenuation on gross earth models, *J. geophys. Res.*, in press.

Isacks, B. & Molnar, P., 1971. Distribution of stresses in the descending lithosphere from a global survey of focal-mechanism solutions of mantle earthquakes, *Rev. Geophys. Space Phys.*, **9**, 103–174.

Jordan, T. H., 1975a. Lateral heterogeneities and mantle dynamics, *Nature*, **257**, 745–750.

Jordan, T. H., 1975b. The continental tectosphere, *Rev. Geophys. Space Phys.*, **13**, (4), 1–12.

Kanamori, H., 1970. Velocity and *Q* of mantle waves, *Phys. Earth planet. Int.*, **2**, 259–275.

Kanamori, H. & Abe, K., 1968. Deep structure of Island Arcs as revealed by surface waves, *Bull. earthq. Res. Inst. (Tokyo)*, **46**, 1001–1025.

Katsumata, M., 1970. Seismicity and some related problems in and near the Japanese Islands, *Kenshin Jiho* (Q. J. seism. Jap. meteor. Agency), **35**, 75–142 (in Japanese).

Kausel, E. G., Leeds, A. R. & Knopoff, L., 1974. Variations of Rayleigh wave phase velocity across the Pacific Ocean, *Science*, **186**, 139–141.

Leeds, A. R., 1975. Lithospheric thickness in the Western Pacific, *Phys. Earth planet. Int.*, **11**, 61–64.

Leeds, A. R., Kausel, E. G. & Knopoff, L., 1974. Variations of upper mantle structure under the Pacific Ocean, *Science*, **186**, 141–143.

Liu, H. P., Anderson, D. L. Kanamori, H., 1976. Velocity dispersion due to anelasticity; implications for seismology and mantle composition, *Geophys. J. R. astr. Soc.*, **47**, 41–58.

Madariaga, R. & Aki, K., 1972. Spectral splitting of toroidal free oscillations due to lateral heterogeneity of the Earth's structure, *J. geophys. Res.*, **77**, 4421–4431.

Noponen, I., 1966. Surface wave phase velocities in Finland, *Bull. seism. Soc. Am.*, **56**, 1093–1104.

Okal, E. A. & Anderson, D. L., 1975. A study of lateral inhomogeneities in the upper mantle by multiple *ScS* travel-time residuals, *Geophys. Res. Lett.*, **2**, 313–316.

Parker, R. L. & Oldenburg, D. W., 1973. Thermal model of an ocean ridge, *Nature Phys. Sci.*, **242**, 137–139.

Sipkin, S. A. & Jordan. T. H., 1975. Lateral heterogeneity of the upper mantle determined from the travel times of *ScS*, *J. geophys. Res.*, **80**, 1474–1484.

Sipkin, S. A. & Jordan, T. H., 1976. Lateral heterogeneity of the upper mantle determined from the travel times of multiple *ScS*, *J. geophys. Res.*, **81**, 6307–6320.

Toksöz, M. N. & Anderson, D. L., 1966. Phase velocities of long-period surface waves and structure of the upper mantle; 1: great circle Love and Rayleigh wave data, *J. geophys. Res.*, **71**, 1649–1658.

Toksöz, M. N. & Ben-Menahem, A., 1963. Velocities of mantle Love and Rayleigh waves over multiple paths, *Bull. seism. Soc. Am.*, **53**, 741–764.

Toksöz, M. N., Minear, J. W. & Julian, B. R., 1971. Temperature field and geophysical effects of a down-going slab, *J. geophys. Res.*, **76**, 1113–1138.

Utsu, T., 1967. Anomalies in seismic wave velocity and attenuation associated with a deep earthquake zone, *J. Fac. Sci. Hokkaido Univ., Ser. 7 (Geophys.)*, **3**, 1–25.

Contribution 2805, Division of Geological and Planetary Sciences, California Institute of Technology.